

# Applications of XPS on Nanoscale Material Research

Fen Liu,<sup>\*</sup> Zhijuan Zhao, Limei Qiu, Liangzhong Zhao

Institute of Chemistry, Chinese Academy of Sciences, Beijing 100080, PR China,

<sup>\*</sup>fenliu@iccas.ac.cn

(Received: November 21, 2008; Accepted: February 17, 2009)

My group has recently been engaged in the following research work on the nanoscale materials by using XPS:

## 1. Evidence of a Unique Electron Donor-Acceptor Property for Platinum Nanoparticles as Studied by XPS

A fundamental question for polymer-stabilized metal nanoparticles is the interaction of the stabilizer with the nanoparticles. Another open question is whether the nanoparticles can possess a distinct property relative to the bulk metal in the interaction. However, to our knowledge, studies on the interaction of the stabilizer with Pt nanoparticles as well as the effect of the interaction on the core-level binding energies (BEs) of the nanoparticles are limited, although the interaction may affect the properties of the nanoparticles. In our work, the chemical interaction of Pt nanoparticles with the stabilizer poly(Nvinyl-

2-pyrrolidone) (PVP) in the solid state is examined and compared with that of bulk Pt metal on the basis of core-level XPS measurements. It is found that Pt atoms in nanoparticles between 2 and 7 nm in size act as electron acceptors whereas Pt atoms in bulk Pt as well as in Pt nanoparticles >25 nm in size act as electron donors in interactions with PVP.

In the interaction of PVP with Pt nanoparticles <7 nm in size, charge transfer is from carbonyl groups in PVP to Pt nanoparticles, whereas in the interaction of PVP with bulk Pt or Pt nanoparticles >25 nm in size, charge transfer is from Pt metal to the polymer side chain of PVP. There exists a critical nanoparticle size between 7 and 25 nm that would lead to a switch in the electron donor-acceptor property.

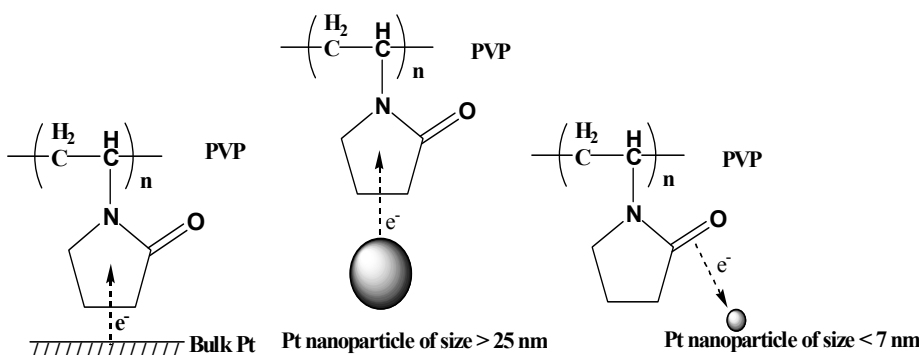


**Fig. 1** The sketch-map of the electron donor-acceptor property.

## 2. Comparative XPS study of surface reduction for nanocrystalline and microcrystalline ceria powder

Nanoscale materials have attracted great interest because of their distinct properties. By means of XPS, we have investigated the difference of reduction behavior between nanocrystalline and microcrystalline ceria on condition of  $Ar^+$  bombardment or X-ray irradiation. For the first time, the results indicate that the reduction level of  $Ce^{4+}$

to  $Ce^{3+}$  is lower for nanocrystalline ceria than for microcrystalline ceria although the experimental conditions are identical. These differences have been attributed to the differences in the concentration of oxygen vacancies in the bulk and the diffusion ability of oxygen atoms between them. It is obvious that nano-ceria has a higher original concentration of the oxygen vacancies than micro-ceria, which provides the more natural path for oxygen diffusion from the inner zone to the

surface region. As a results the observed reduction level is lower for nano-ceria than for micro-ceria

within the information depth of XPS.

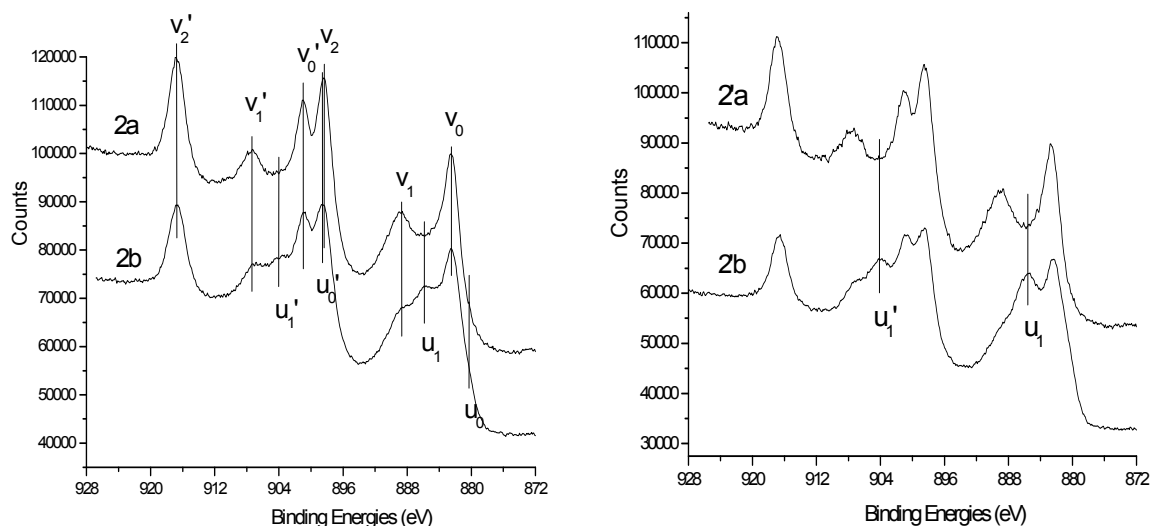


**Fig. 2 and 2'** Ce3d XPS spectra from nano-ceria (2) and micro-ceria (2')  
 a) Before Ar<sup>+</sup> bombardment;  
 b) Sputtered with 3 keV Ar<sup>+</sup> at ca. 5  $\mu\text{A}\cdot\text{cm}^{-2}$  for 6 min.

### 3. Core Level Binding Energy Shifts Caused by Size Effect of Nanoparticles

XPS spectra were used to determine the binding energies for Pt-PVP nanoparticles before and after Ar<sup>+</sup> ion sputtering, as well as for some oxides nanoparticles (TiO<sub>2</sub>, ZnO, and SiO<sub>2</sub>). The binding energies of the nanoparticles were compared with those of the corresponding bulk materials. The results showed that, compared with bulk Pt, the Pt4f binding energy of Pt-PVP nanoparticles before Ar<sup>+</sup> ion sputtering shifted to lower binding energy side.

After Ar<sup>+</sup> sputtering, the PVP on Pt nanoparticles was sputtered away and the Pt nanoparticles became bare, the binding energy shifted to higher binding energy side. By comparison with the bulk oxides, the binding energies of TiO<sub>2</sub>, ZnO, and SiO<sub>2</sub> nanoparticles also shifted to the higher binding energy side, and the magnitude of binding energy shift was in the order of TiO<sub>2</sub><ZnO<SiO<sub>2</sub>. The effect of extra-atomic relaxation was used to explain the binding energy shift of nanoparticles.

**Table 1** Pt 4f<sub>7/2</sub> binding energies of Pt-PVP nanoparticles and bulk Pt.

Sample	Size of Pt nanoparticles (nm)	R <sup>a</sup>	Pt 4f <sub>7/2</sub> binding energy (eV)		
			before Ar <sup>+</sup> sputtering	after Ar <sup>+</sup> sputtering <sup>b</sup>	after Ar <sup>+</sup> sputtering <sup>c</sup>
1	2-3	2	70.6	71.7	72.2
2	2-3	10	70.7	71.5	72.1
3	2-3	20	70.8	72.0	72.4
4	2-3	50	70.6	72.1	72.2
5	bulk Pt		71.0		

(a) R: the molar ratio of PVP (as a monomeric unit) to Pt in the precursor solution; (b) calibration of binding energy using amorphous carbon (C 1s=284.4 eV) produced by Ar<sup>+</sup> sputtering; (c) calibration of binding energy using Ar atoms (Ar 2p<sub>3/2</sub>=241.5 eV) implanted during Ar<sup>+</sup> sputtering.

**Table 2** Core level binding energies of nanosize oxides and the corresponding bulk oxides.

Oxides	Core level	Binding energy of nanosize oxides (eV)	Binding energy of bulk oxides (eV)	Binding energy shifts (eV)
TiO <sub>2</sub>	Ti 2p <sub>3/2</sub>	458.68	458.54	0.14
ZnO	Zn 2p <sub>3/2</sub>	1021.53	1021.27	0.26
SiO <sub>2</sub>	Si2p	103.57	103.17	0.40

#### 4. XPS Study of BiI<sub>3</sub>-Nylon 11 Nanocomposites

The chemical states of Bi in BiI<sub>3</sub>-nylon 11 nanocomposites during X-ray irradiation were investigated by X-ray photoelectron spectroscopy (XPS). It has been found that with prolonging exposure to Mg K $\alpha$  X-ray, Bi 4f peak of Bi metallic state emerged at lower binding energy side and the peak intensity continuously increased; while Bi 4f peak intensity of BiI<sub>3</sub> gradually decreased. Under the same XPS experimental conditions, the reduction level of BiI<sub>3</sub> to metallic Bi is much higher for BiI<sub>3</sub>-nylon 11 nanocomposite than for bulk BiI<sub>3</sub>. The reduction behavior of Bi in BiI<sub>3</sub> of

nanocomposite induced by X-ray may play an important role for the X-ray photoconductivity. The XPS results also show that BiI<sub>3</sub>-nylon 11 nanocomposite has a smaller charging shift than those of pure nylon 11 and bulk BiI<sub>3</sub> under the same experimental conditions, and the charging shift of BiI<sub>3</sub>-nylon 11 nanocomposite decreasing with increasing X-ray exposure time. This phenomenon may be used to inspect the X-ray photoconductivity. Besides, the N 1s and O 1s binding energies of pure nylon 11 are smaller than those of BiI<sub>3</sub>-nylon 11 nanocomposite due to the coordination of BiI<sub>3</sub> with the amide linkages of nylon 11.

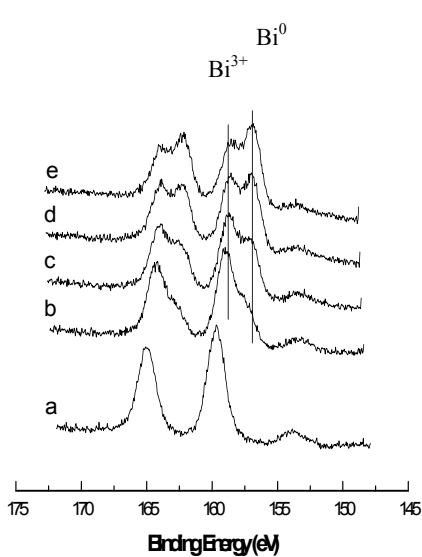


**Fig. 3** Bi 4f spectra of BiI<sub>3</sub>-nylon 11 nanocomposite film exposed to Mg K $\alpha$  X-ray irradiation for different durations:  
a) 2 min, b) 0.5 h, c) 1.0 h, d) 1.5 h, e) 2.0 h.

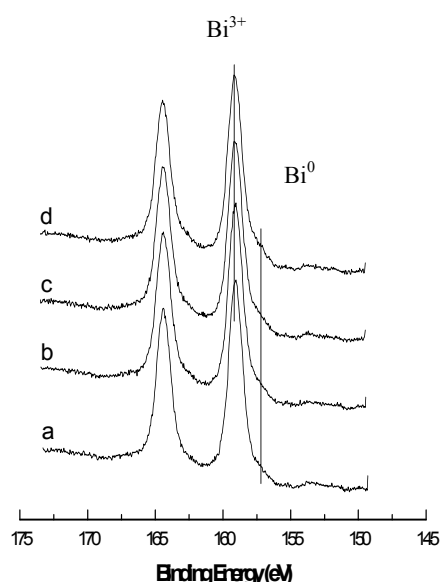


**Fig. 4** Bi 4f spectra of bulk BiI<sub>3</sub> powder samples with exposure to Mg K $\alpha$  X-rays for different durations: a) 2 min, b) 0.5 h, c) 1.0 h, d) 1.5 h.